

1 Essential Role of Eclosion Hormone
2 Precursor and Receptor Genes in Desert
3 Locust Ecdysis
4

5 Lina Verbakel^{1,2}, Cynthia Lenaerts¹, Jerom Vranken¹, Elisabeth Marchal^{1,3} and Jozef Vanden Broeck^{1*}

6 ¹Molecular Developmental Physiology and Signal Transduction, Biology Department, KU Leuven,
7 Naamsestraat 59 box 2465, B-3000 Leuven, Belgium.

8 ²Present address: Nagi Bioscience SA, EPFL Innovation Park (M), Rue des Jordils 1A 1025 Saint-
9 Sulpice, Switzerland.

10 ³Present address: Imec, Kapeldreef 75, B-3001 Leuven, Belgium

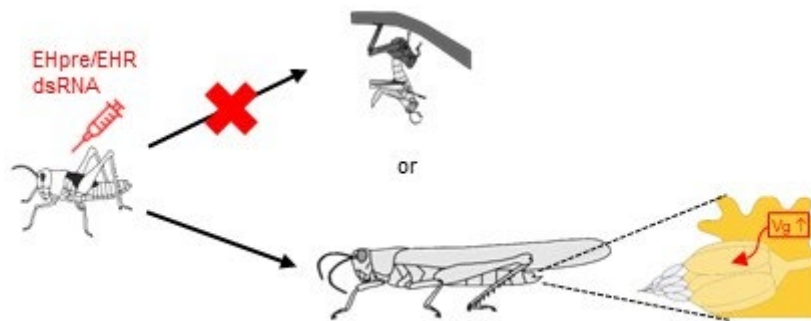
11 ***Correspondence:** Jozef Vanden Broeck, Molecular Developmental Physiology and Signal
12 Transduction, Biology Department, KU Leuven, Naamsestraat 59 box 2465, B-3000 Leuven, Belgium.

13 **Email:** jozef.vandenbroeck@kuleuven.be

14

15

16 **Graphical Abstract**



17

18 **Abstract**

19 The process of molting represents a critical phase in the life cycle of arthropods, marking periods of
20 growth and development. Central to this process is the eclosion hormone (EH), a neurohormone that
21 plays a pivotal role in initiating and regulating the complex sequence of events leading to successful
22 molting in holometabolan species. Very little information is available in Hemimetabola, which display
23 a different kind of development characterized by gradual changes. This paper reports on the
24 identification of the two EH precursors and the EH receptor (EHR), a guanylyl cyclase, in a
25 hemimetabolan pest species, the desert locust, *Schistocerca gregaria*. Using qRT-PCR, an in-depth
26 profiling study of *Schgr*-EH-1, -2 and *Schgr*-EHR transcripts was performed. Silencing of *Schgr*-EH-1, -2
27 and *Schgr*-EHR resulted in lethality at the expected time of ecdysis, thereby showing their crucial role
28 during this process.

29

30 **Keywords**

31 Hemimetabola, insect, knockdown, molt, neuropeptide, Eclosion Hormone

32

33 **Highlights**

34 -Identification of *Schgr*-EH and *Schgr*-EHR transcripts in the desert locust

35 -Expression profiling of *Schgr*-EH and *Schgr*-EHR transcripts in the desert locust

36 -*Schgr*-EH and *Schgr*-EHR are essential for ecdysis in *Schistocerca gregaria*

37 -Knockdown led to some nymphs molting into a supernumerary instar

38 -Knockdown led to some nymphs molting into adults with expedited vitellogenesis

39 1. Introduction

40 The success story of insects is in large part due to their exoskeleton, a robust armor that shields them
41 from dehydration and other environmental threats, while also serving as a scaffold for muscle
42 attachment. This exoskeleton, however, necessitates periodic shedding through molting cycles to
43 accommodate growth, culminating in the critical phase of ecdysis, the shedding of the old cuticle. This
44 transition is not merely a physical transformation but the result of a complex interplay of hormonal
45 and neuropeptidergic signals ensuring the seamless progression vital for their survival¹⁻³.

46 Central to this orchestration is the Eclosion Hormone (EH), first identified as a pivotal factor in initiating
47 eclosion in various lepidopteran species⁴. Subsequent studies expanded the existing knowledge of EH,
48 revealing its presence and sequence in a range of insects, underscoring its ubiquity and importance
49 across taxa⁵⁻⁷. EH's role was shown to be particularly pronounced during pupation in holometabolous
50 species such as *Manduca sexta* and *Drosophila melanogaster*, where it triggers a surge in intracellular
51 cyclic GMP (cGMP) levels⁸. Furthermore, two isoforms of an EH receptor (EHR) belonging to the
52 receptor guanylyl cyclase family have been characterized in the Oriental fruit fly, *Bactrocera dorsalis*;
53 *i.e.*, *BdmGC-1* and *BdmGC-1β*^{8,9}.

54 The regulation of ecdysis is highly coordinated and involves not only EH but also other neuropeptides,
55 such as the ecdysis-triggering hormone (ETH), as well as ecdysteroids, the arthropod steroid hormones.
56 Ecdysteroids play a pivotal role in initiating molting cycles and orchestrating the downstream
57 neuropeptide signaling cascade that prepares the insect for ecdysis. In *M. sexta*, ETH is produced by
58 Inka cells, specialized glandular cells that are closely associated with the tracheal system, and acts in
59 tandem with EH to trigger motor patterns required for shedding the old cuticle¹⁻³. Binding of EH to its
60 receptor on Inka cells has been shown to stimulate the release of ETH, which then activates central
61 and peripheral neural circuits that drive the suite of ecdysis behaviors^{10,11}. These interconnected
62 pathways highlight the involvement of multiple tissues, including the central nervous system (CNS) and
63 the tracheal system, in the regulation of ecdysis.

64 Despite the clear involvement of EH in the ecdysis of lepidopteran species, such as *Bombyx mori* and
65 *M. sexta*, its role across different insect orders remains complex and varied. In coleopterans, such as
66 *Tribolium castaneum*, EH signaling is crucial for ecdysis¹², and more recent studies in *Drosophila*
67 *melanogaster* have confirmed that EH also plays a vital role in initiating ecdysis by priming the nervous
68 system to respond to ETH¹³. However, earlier studies suggested a more nuanced role for EH in *D.*
69 *melanogaster*, with some mutants displaying only minor behavioral deficits^{1-3,14}. This variability
70 highlights that, while EH is essential for ecdysis in all studied species, the extent of its functional
71 contribution and its integration with other signaling pathways can differ significantly across insect taxa.

72 These findings illustrate the multifaceted nature of EH signaling in regulating ecdysis across the class
73 of insects.

74 The current study extends the exploration of EH's role in ecdysis to the desert locust, *Schistocerca*
75 *gregaria*, a hemimetabolan (orthopteran) species that stands out for its remarkable population
76 density-dependent phenotypic plasticity and its devastating impact on agriculture caused by huge
77 migrating swarms¹⁵. Here, we report on the molecular characterization of two EH precursors and a
78 putative EH receptor in this locust species, shedding light on their sequence conservation across hemi-
79 and holometabolan species. In addition, temporal profiling of EH precursor and receptor transcripts
80 was performed at various time points throughout the fifth nymphal instar (N5). Finally, we
81 demonstrate a crucial role for the *S. gregaria* EH signaling system in ecdysis of *S. gregaria* by utilizing
82 RNA interference (RNAi). Our findings not only contribute to the broader understanding of ecdysis
83 regulation but may also have potential implications for controlling locust outbreaks.

84 2. Materials and Methods

85 2.1. Insect rearing and tissue sampling

86 The desert locusts (*S. gregaria*) were reared under crowded conditions at a temperature of 30 ± 1 °C,
87 with a relative humidity between 40-60% and a photoperiod of 14h. For gene expression analysis by
88 qRT-PCR, tissues were sampled from female hoppers that were collected in the fifth nymphal instar
89 and dissected at various time points: immediately after molting (N5D0), two and four days after the
90 molt (N5D2 and N5D4, respectively), at an inter-wing distance of at least 1.8 mm (N5IW, which
91 corresponds to the time of the ecdysteroid peak approximately three days before the adult molt), at
92 the time of the weight peak (N5WP, corresponding approximately to two days before the adult molt),
93 and at the time of the weight drop (N5WD, corresponding approximately to one day before the adult
94 molt). These developmental time points were previously described in detail by Verbakel et al. (2021)¹⁶.
95 Tissues were collected in 5 independent pools of 3 animals each.

96 2.2. RNA extraction, cDNA synthesis and qRT-PCR

97 RNA extraction and subsequent complementary DNA (cDNA) synthesis and quantitative real-time PCR
98 (qRT-PCR) from brain, abdominal ganglia, and trachea tissues were performed as previously
99 described¹⁶. In brief, lipid rich tissues such as brains¹⁶ and abdominal ganglia were extracted using the
100 Qiagen® RNeasy Lipid Tissue Kit, including the DNase digestion protocol (RNase-Free DNase set,
101 Qiagen), and trachea were extracted using the RNAqueous-Micro Kit (Ambion). Both kits were utilized
102 according to manufacturer's protocol. cDNA was generated from 500 ng extracted RNA using the
103 PrimeScript™ reagent kit (Takara Bio Inc.) and further diluted ten-fold in sterile water (Milli-Q,
104 Millipore). The transcript levels of the genes of interest were analyzed with qRT-PCR using the Fast

105 SYBR[®] Green Master Mix (Applied Biosystems) and oligonucleotide primers (Table S1), following the
106 protocol previously described by Verbakel et al., (2021)¹⁶. Each primer pair that was utilized for qRT-
107 PCR profiling of the *S. gregaria* EH precursor (*Schgr-EHpre-1* and *-2*) and receptor (*Schgr-EHR*)
108 transcripts (Table S1) was validated as previously described¹⁶. However, it is important to note that the
109 primers for detecting the *S. gregaria* EH precursor transcripts in this study were designed based on
110 conserved sequence regions and, consequently, do not differentiate between the *Schgr-EHpre-1* and
111 *Schgr-EHpre-2* isoforms. As a result, the expression levels reported represent the combined expression
112 of both (very similar) isoforms. Amplification efficiency and specificity were confirmed by melting curve
113 analysis, agarose gel electrophoresis and sequencing. All qRT-PCR results were calculated according to
114 the comparative $\Delta\Delta C_t$ method¹⁷. GraphPad Prism (GraphPad Software Inc. version 6.3) was used to
115 plot and transform the data using the following equation: $Y = \log(Y)$, after which the statistical
116 significance was tested. First normality was determined using the Shapiro-Wilk test. If $n < 3$, normality
117 was assumed. Finally, to evaluate the statistical significance, an ANOVA followed by a Dunnett's test
118 or a student's t-test was used. When $n > 3$, data were statistically evaluated by the non-parametric
119 Mann-Whitney U test.

120 **2.3. Molecular cloning of *Schgr-EHpre-1*, *Schgr-EHpre-2* and putative *Schgr-EHR***
121 The complete open reading frames (ORFs) of *Schgr-EHpre-1*, *Schgr-EHpre-2* and putative *Schgr-EHR*,
122 were acquired by tBLASTn analysis using the most recently curated *S. gregaria* transcriptome and
123 genome data¹⁸ (transcript SCHGR_00013205, SCHGR_00000893 and SCHGR_00006115 from locus
124 104602-168818, 1311805-132056 and 557220-758965 of the seq7654, seq342 and seq7753 contig,
125 respectively). To this end, the amino acid sequence of *M. sexta* EHpre (Genbank accession number:
126 AAA29331.1) was used as a query for both *Schgr-EHpre*, *Schgr-EHpre-1* and *-2*, while the amino acid
127 sequence of *B. dorsalis* GC-1 β (Genbank accession number: ACQ90240.1) was used as a query for
128 *Schgr-EHR*. Primers specific to the hit regions are depicted in Table S1. The resulting PCR amplicon
129 sequences were verified by Sanger sequencing (LGC Genomics GmbH).

130 **2.4. RNA interference**
131 The *dsRNA* constructs that target either *Schgr-EHpre-1/-2* or *Schgr-EHR* were prepared according to
132 the previously described approach¹⁶. In brief, oligonucleotide primers with a T7 promoter overhang
133 (Table S1) were used to generate *dsRNA* constructs and the Ambion's MEGAscript[®] RNAi Kit, following
134 the procedures described by Verbakel et al. (2021)¹⁶. The *dsRNA* constructs designed for targeting the
135 *S. gregaria* EH precursor transcripts do not differentiate between the isoforms, as both *dsRNA*
136 constructs target a conserved region common to both *Schgr-EHpre* transcripts. This means that any
137 knockdown effects observed reflect the combined impact on both isoforms. The primers used to
138 construct the different *dsRNA* constructs are listed in Table S1. Each construct was diluted (100 ng/ μ L)

139 in *S. gregaria* saline ((1 L: 8.766 g NaCl; 0.188 g CaCl₂; 0.746 g KCl; 0.407 g MgCl₂; 0.336 g NaHCO₃;
140 30.807 g sucrose; 1.892 g trehalose). The injection schemes were conducted in *S. gregaria* nymphs to
141 elucidate the role of the EH(R) signaling system in ecdysis. Fourth instar nymphs (N4) received a first
142 injection (4μL) at the day of the molt (N4D0). Boost injections were conducted at N4D3, N5D1 and
143 N5D5. Nymphs were injected into the hemocoel with each respective construct or with a combination
144 of *dsEH(pre/R)* constructs. Control locusts were injected with *dsGFP*. To test RNAi knockdown
145 efficiency, tissues of five individual animals were collected at N5D4.

146 3. Results

147 3.1. The *Schgr*-EH sequences show sequence similarity to characterized insect 148 EH sequences

149 The *Schgr-EHpre-1* and *-2* ORF sequences consist of, respectively, 261 and 252 nucleotides encoding
150 prepropeptides of, respectively, 86 and 83 amino acids (Figure 1), with an N-terminal hydrophobic
151 signal peptide of, respectively, 30 and 28 amino acids long, as predicted by SignalP-5.0¹⁹. A multiple
152 sequence alignment reveals that both mature *Schgr*-EH peptide sequences show a high identity to
153 characterized EH sequences of other insect species, including six highly conserved cysteine residues
154 (Figure 1). The *Schgr*-EH1 sequence is 74.14% and 77.59% similar to *Drome*-EH and *Bacdo*-EH
155 sequences, respectively, and 72.41% and 74.14% similar to *Manse*-EH and *Bommo*-EH sequences,
156 respectively. The similarity between *Schgr*-EH2 sequence and *Drome*-EH, *Bacdo*-EH, *Manse*-EH and
157 *Bommo*-EH sequences is 72.41%, 75.86%, 70.69% and 70,69%, respectively. The *Schgr*-EH1 and EH2
158 isoforms share a high degree of similarity, 89.28%. Due to this high level of sequence conservation, we
159 were not able to design qRT-PCR primers nor dsRNA constructs that distinguish between the two
160 isoforms, resulting in a combined measurement of their expression levels and effects.

161 3.2. The putative *Schgr*-EHR shows sequence similarity to the characterized 162 EHRs of *B. dorsalis*

163 The open reading frame of the putative *Schgr*-EHR encodes a polypeptide of 1432 amino acids (Figure
164 2). Protein domain prediction identified the putative *Schgr*-EHR as a membrane guanylyl cyclase (mGC)
165 with an extracellular ligand-binding domain (ECD; amino acids 32-492), a hydrophobic transmembrane
166 region (TM; amino acids 488-510), a regulatory pseudokinase-homology domain (PKHD; amino acids
167 541-828), an adenylyl-/guanylyl cyclase catalytic domain c (CYCc; amino acids 861-1054) and a
168 carboxyl-terminal extension of 378 residues. The alignment (Figure 2) to both *Bacdo*-EHR sequences,
169 *BdmGC-1* and *BdmGC-1β*, reveals the presence of conserved PTFARTXPPDTQ (amino acids 139-150)
170 and AAYLYDAVXLYAXALXXVL (amino acids 350-372) motifs in the ECD, as well as high sequence
171 similarity in the PKHD (58.03%) and CYCc (82.99%) domains. The overall sequence similarity of *Schgr*-
172 EHR with *BdmGC-1* and *BdmGC-1β* is 47.36% and 44.22%, respectively.

173 3.3. Temporal profiling of *Schgr-EH* precursor and receptor transcripts

174 In the brain, the levels of the *Schgr-EHpre* transcripts (Figure 3A) showed no significant differences
175 between the timepoints analyzed throughout the fifth instar. Similarly, in the trachea, the expression
176 levels of the putative EH receptor (*Schgr-EHR*) transcript remained consistent across the same
177 timepoints, suggesting stable expression in this tissue during this developmental stage (Figure 3B). By
178 contrast, a significant increase in the *Schgr-EHR* transcript levels was observed in the abdominal ganglia
179 at N5WD compared to earlier timepoints during the intermolt phase, specifically N5D0 and N5D2
180 (Figure 3C).

181 3.4. Developmental effects of *Schgr-EH* precursor or receptor depletion

182 3.4.1. Knockdown efficiency

183 The knockdown efficiency of the *dsEHpre* (*-a* and *-b*) and *dsEHR* constructs was assessed. The *dsEHpre-*
184 *a* construct significantly reduced the combined levels of both *Schgr-EHpre-1* and *Schgr-EHpre-2*
185 transcripts in brain tissues dissected at N4D4 and N5D4 by 86 % and 83 %, respectively (Figure S1A, C).
186 Likewise, the *dsEHpre-b* construct significantly reduced the combined levels both *Schgr-EHpre-1* and
187 *Schgr-EHpre-2* transcripts in brain tissues dissected at N4D4 and N5D4 by 86 % and 87 %, respectively.
188 While the *dsEHR* construct did not yet cause a knockdown in the trachea at N4D4, the *Schgr-EHR*
189 transcript levels were significantly reduced by 40 % in the trachea at N5D4 (Figure S1B, D).

190 3.4.2. Ecdysis defects observed

191 Administering *dsEHpre-b* and/or *dsEHR* constructs through injections led to most nymphs failing to
192 complete pre-ecdysis or ecdysis successfully. Approximately 22%, 2% and 31% of the *Schgr-EHpre-*,
193 *Schgr-EHR-* and *Schgr-EH(pre/R)* depleted nymphs, respectively, were arrested during pre-ecdysis or
194 ecdysis in the last nymphal-nymphal (N4-N5) molt, while the rest and the control *dsGFP*-injected
195 nymphs successfully molted to the last nymphal instar (Figure 4A). At the nymphal-adult (N5-Ad) molt,
196 another 58%, 78% and 53% of the *Schgr-EHpre-*, *Schgr-EHR-* and *Schgr-EH(pre/R)* depleted nymphs,
197 respectively, were not able to successfully complete ecdysis, whereas the *dsGFP*-injected control
198 nymphs all achieved successful N5-Ad molts (Figure 4A). The *Schgr-EH-*, *Schgr-EHR-* or *Schgr-EH(pre/R)*
199 depleted nymphs attained a pinkish color right before the onset of ecdysis, which was also observed
200 in *dsGFP*-injected control nymphs. However, in contrast to the control nymphs that successfully
201 completed the ecdysis process, the *Schgr-EHpre* and/or *Schgr-EHR* depleted nymphs either darkened
202 and died without completing ecdysis (Figure 4A) or showed developmental deficits with signs of
203 physical weakening, such as reduced mobility and loss of postural control, before succumbing (Figure
204 4B). These phenotypes were consistently associated with developmental ecdysis deficits (Figure 4A
205 and 4B). The rest of the *Schgr-EHpre-*, *Schgr-EHR-* and *Schgr-EH(pre/R)* depleted nymphs (20%, 20%
206 and 16%, respectively) molted into instantly beige-yellowish colored adult locusts, while the newly

207 ecdysed *dsGFP*-injected control locusts still had a normal, more pinkish appearance. The beige-
208 yellowish *dsEHpre-b* and/or *dsEHR*-injected locusts displayed a similar physical body size and wings as
209 the control fledglings (Figure 4C). It must, however, also be noted that the coloration of the *Schgr-*
210 *EHpre* and/or *Schgr-EHR* depleted adult locusts was dissimilar from the (bright) yellow coloration
211 observed in mature adult male locusts²⁰. It is also worth mentioning that in a few rare cases *EHpre/EHR-*
212 depleted nymphs molted into a supernumerary nymphal (N6) instar (Figure 4D).

213 Adult female locusts that developed from nymphs injected with *dsEHpre* or *dsEHR* already exhibited
214 full vitellogenesis 10 days after the final molt, in contrast to the control group females, which were just
215 initiating this process. Specifically, experimental females from the *Schgr-EHpre-* and *Schgr-EHR* RNAi
216 treatment groups showed average oocyte lengths of 4.4 mm and 4.9 mm, respectively, compared to
217 the average of 2.3 mm in the *dsGFP*-injected control group (Figure 5).

218 4. Discussion

219 Consistent with previously characterized EH peptides, the two predicted *Schgr-EH* peptides exhibit a
220 conserved structure, featuring six highly conserved cysteine residues that are likely to form three
221 intramolecular disulphide bonds. These bonds are posited to be crucial for the biological activity of
222 EH^{21,22}. Furthermore, computational predictions have identified two EH isoforms in various other insect
223 species, including *Nilaparvata lugens* (the brown planthopper, Hemiptera), *Danaus plexippus* (the
224 monarch butterfly, Lepidoptera), *Diaphorina citri* (the Asian citrus psyllid, Hemiptera), *Locusta*
225 *migratoria* (the migratory locust, Orthoptera), and *Tribolium castaneum* (the red flour beetle,
226 Coleoptera)²³. The two putative *EHpre* isoforms have been identified in specific loci in the recently
227 published genome sequence database of *S. gregaria*¹⁸. Some neuropeptide precursor genes have been
228 shown to have undergone several duplications, including eclosion hormone. Noteworthy is the
229 phylogenetic tree analysis conducted by Veenstra in 2014, which suggested that in some instances,
230 such as in *L. migratoria* and *D. plexippus*, a relatively recent gene duplication event may have occurred,
231 whereas in other species, gene duplication was inferred to have taken place much earlier²².

232 One putative *EHR* was found in the *S. gregaria* genome database¹⁸ and it exhibits several common
233 characteristics with both characterized EH receptor isoforms of *B. dorsalis*^{8,9}. Specifically, the putative
234 *Schgr-EHR* shows all features of receptor guanylyl cyclases. Sequence alignment revealed two
235 conserved cysteine residues (C₁₁₁ and C₁₃₀) in their extracellular domain, which will probably form
236 intrachain disulphide bonds that are critical for ligand-binding affinity of receptor guanylyl cyclases²⁴.
237 Moreover, the cysteine pairs (C_{205,206} and C_{212,213}) are likely to play a role in mGC receptor dimerization
238 through interchain disulphide bonds, as this phenomenon is known to increase ligand-binding affinity
239 of mammalian guanylyl cyclases²⁵. In addition, the two proposed conserved extracellular domain

240 motifs might be indicative for crucial amino acid residues in ligand-receptor interaction and/or for
241 structural configurations of the receptor. For example, the AAYLYDAVXLYAXALXXVL motif is
242 hydrophobic, yet also contains some polar and charged amino acids, which is a prerequisite for the
243 ligand-binding domain that often constitutes a hydrophobic-binding pocket that attracts and may bind
244 the ligand through polar interactions²⁶. The PTFARTXPPDTQ motif, on the other hand, is proline-rich
245 and might play a role in the configuration of the receptor and influence its cellular signaling²⁷.
246 Confirmation of these suggestions would require more detailed structural analysis and mutagenesis
247 studies, which is out of the scope for our research.

248 Like *BdmGC-1* and in contrast to *BdmGC-1 β* , the putative *Schgr-EHR* possesses a long and unique C-
249 terminal tail with an unidentified function⁸. In mammalian sensory organ guanylyl cyclases, the
250 prolonged C-terminal tail is thought to be involved in interactions with cytoplasmic proteins, such as
251 the cytoskeleton²⁴. Typically, the amino-terminal region of mammalian guanylyl cyclases contains a
252 heme-binding domain and a carboxyl-terminal catalytic domain, which is also observed in the *Schgr-*
253 *EHR* sequence. Their activation requires an intermediate messenger, such as nitric oxide (NO) or
254 carbon monoxide (CO), which binds the heme group and may serve as a hub for receptor
255 dimerization²⁴.

256 At present, it is unknown if the putative *Schgr-EHR* can indeed be activated by *Schgr-EH-1* and/or *-2*,
257 in a similar way as described for both *BdmGC-1* and *BdmGC-1 β* ^{8,9}. However, the presented evidence
258 suggests important parallels between *Schgr-EHR* and the characterized *B. dorsalis* EH receptors, such
259 as the pronounced sequence similarity of *Schgr-EHR* with *BdmGC-1*⁹ and the ecdysis defects that
260 resulted from the functional knockdown.

261 This study showed that depletion of *Schgr-EHpre-1/-2* and/or *Schgr-EHR* transcripts resulted in severe
262 suppression of (pre-)ecdysis during the incomplete metamorphosis of the vast majority of the
263 experimentally treated locusts. EH has been implicated in the functional control of ecdysis and
264 metamorphosis in multiple holometabolan insect species¹⁻³. In addition, EH release from the
265 neurohemal sites has been observed prior to ecdysis in both *M. sexta*²⁸ and *B. mori*^{6,29}. Moreover,
266 exposure of isolated CNS to *Manse-EH* induced the ecdysis motor program in *M. sexta*². In addition, *D.*
267 *melanogaster eh* null mutants failed to express pre-ecdysis and ecdysis behaviors¹³. However, by
268 contrast, older literature in *D. melanogaster* stated that EH was solely vital for the execution of
269 eclosion^{1,2,14}. *Trica-EHpre* depleted *T. castaneum* also displayed severe weakening of pre-ecdysis and
270 complete suppression of ecdysis¹².

271 In contrast to what has been reported in *D. melanogaster* (Diptera)⁵ and *Heortia vitessoides*
272 (Lepidoptera)³⁰, the transcript levels of *Schgr-EHpre-1/-2* did not dramatically increase prior to ecdysis

273 in *S. gregaria* brain tissues, at least not at the measured time points. The transcript levels of the
274 putative *Schgr-EHR* also remained relatively stable in the tracheal tissues, which house the Inka cells,
275 specialized glandular cells responsible for production and secretion of the ecdysis-triggering hormone
276 (ETH)², whereas in the abdominal ganglia a significant increase in *Schgr-EHR* transcript levels was
277 observed prior to ecdysis. It has been shown that it is not peripheral, but central EH release that is
278 responsible for EH's role in triggering the ecdysis motor program in *M. sexta*³¹. Moreover, as shown by
279 Kruger et al. (2015), *eh* null mutants (*D. melanogaster*) experienced a diminished responsiveness to
280 ETH in the 27/704 neurons that express crustacean cardioactive peptide (CCAP), which are critical for
281 the downstream activation of the ecdysis motor program¹³. This indicated that, at least in *D.*
282 *melanogaster*, EH is crucial for priming the nervous system to respond to ETH, with both EH and ETH
283 together setting the stage for the initiation of ecdysis at the end of the molt.

284 Further exploration is warranted to assess a possible necessity of EH and its receptor during the N4-
285 N5 molt in *S. gregaria*. Despite the initiation of *dsRNA* injections in fourth instar nymphs, a mere 20%
286 of the *Schgr-EHpre* depleted nymphs were arrested at the N4-N5 molt, suggesting partial efficacy.
287 Given that EH is a neuropeptide hormone, it is plausible that it accumulates in secretory vesicles
288 located at the axon terminals of neurohemal organs or within other regions of the nervous system. In
289 *M. sexta*, the expression of EH is constitutive, with the ventromedial (VM) neurons projecting their
290 axons throughout the ventral nerve cord and terminating in neurohemal proctodeal nerves on the
291 hindgut surface. These release sites, connected to the CNS via VM neuron projections, are critical for
292 systemic coordination of ecdysis behaviors¹⁻³. Analogously, in adult *D. melanogaster*, VM neurons have
293 been shown to also project to the retro-cerebral complex⁵, a major site of neurohemal release. Hence,
294 it is conceivable that EH reserves were not yet sufficiently exhausted (by the RNAi-mediated
295 knockdown) at the onset of N4-N5 ecdysis, possibly contributing to the observed molting outcomes.

296 Despite the substantial ecdysis-related deficits and nymphal lethality observed in the majority of the
297 population following the depletion of *S. gregaria* EH and/or EHR, a subset of adults managed to
298 emerge, albeit with notable abnormalities. Among these anomalies, the adult females that developed
299 from nymphs injected with *dsEHpre*- and/or *dsEHR* exhibited expedited vitellogenesis and a beige-
300 yellowish hue. A regulatory role in oogenesis for EH has been implicated in the crustacean *Eriocheir*
301 *sinensis* (the chinese mitten crab)³². In addition, a comparative transcriptomic study has shown that
302 EH transcripts are downregulated during ovarian maturation in the crustacean *Litopenaeus vannamei*
303 (the Pacific white shrimp)³³. Furthermore, the occurrence of supernumerary N6 nymphs, albeit rare,
304 alongside the described phenotype, suggests a potential disruption in juvenile hormone (JH) signaling.
305 JH is crucial for the reproductive physiology in adult locusts³⁴⁻³⁶. Notably, JH also induces the
306 expression of the yellow protein, which is involved in the induction of yellow body color (yellowing) in

307 *S. gregaria*^{35,37}. Under crowded conditions, yellowing is particularly pronounced in sexually mature
308 male adults, but to a lesser extent also occurs in aged female adults^{20,37}. In addition, JH's role in
309 maintaining the developmental *status quo* in juvenile insects, by inhibiting metamorphosis, might
310 provide an explanation for the emergence of supernumerary N6 nymphs.

311 5. Conclusion

312 In conclusion, the physiological data reported in this study support the existence of an important
313 regulatory role for EH signaling in the initiation of the ecdysis sequence during the (incomplete)
314 metamorphosis of *S. gregaria* and suggests a possible inhibitory role in ovarian maturation. This finding
315 is imperative as the exact function of peptides in the ecdysteroid-induced neuropeptide cascade differs
316 across species^{1,2}.

317 **CRedit authorship contribution statement**

318 Conceptualization: L.V., C.L., E.M. and J.V.B.; methodology: L.V., JV; validation: L.V. and J.V.B.; formal
319 analysis: L.V.; investigation: L.V., J.V. and C.L.; data curation: L.V.; writing—original draft preparation:
320 L.V. and J.V.B.; writing—review and editing: all authors; supervision: C.L., E.M. and J.V.B.

321 **Declaration of competing interest**

322 The authors declare that they have no known competing financial interests or personal relationships
323 that could have appeared to influence the work reported in this paper.

324 **Data availability**

325 Data will be made available on request.

326 **Acknowledgements**

327 The authors gratefully thank Evelien Herinckx and Arnold Van Den Eynde for taking care of the locust
328 rearing facility. The authors are also very grateful to Emilie Monjon, Paulien Peeters, Heleen Verlinden
329 and Evert Bruyninckx for their useful advice and/or technical assistance.

330 **Funding**

331 This research was funded by the European Union's Horizon 2020 Research and Innovation program
332 [No. 634361 (nEUROSTRESSPEP)], the Special Research Fund of KU Leuven (BOF grant) [C14/19/069],
333 and the Research Foundation of Flanders (FWO) [G090919N], which also provided a PhD fellowship to
334 L.V. [VS.034.16N].

335 6. References

336

- 337 1. White, B. H. & Ewer, J. Neural and hormonal control of postecdysial behaviors in insects. *Annu*
338 *Rev Entomol* **59**, 363–381 (2014).
- 339 2. Žitňan, D. & Adams, M. E. Neuroendocrine Regulation of Ecdysis. L. Gilbert (Ed.), *Insect*
340 *Endocrinology, Elsevier/Academic Press* 253–309 (2012).
- 341 3. Belles, X. Insect metamorphosis, from natural history to regulation of development and
342 evolution, (ISBN: 978-0-12-813020-9) *Elsevier/Academic Press* (2020).
- 343 4. Truman, J. W. & Riddiford L.M. Neuroendocrine control of ecdysis in silkmoths. *Science* **167**,
344 1624–1627 (1970).
- 345 5. Horodyski, F. M., Ewer, J., Riddiford, L. M. & Truman, J. W. Isolation, characterization and
346 expression of the eclosion hormone gene of *Drosophila melanogaster*. *Eur J Biochem* **215**,
347 221–228 (1993).
- 348 6. Kono, T., Nagasawa, H., Isogai, A., Fugo, H. & Suzuki, A. Isolation and complete amino acid
349 sequences of eclosion hormones of the silkworm, *Bombyx mori*. *Insect Biochem* **21**, 185-195
350 (1991).
- 351 7. Marti, T., Takio, K., Walsh, K. A., Terzi, G. & Truman, J. W. Microanalysis of the amino acid
352 sequence of the eclosion hormone from the tobacco hornworm *Manduca sexta*. *FEBS Lett*
353 **219**, 415–418 (1987).
- 354 8. Chang, J.-C., Yang, R.-B., Adams, M. E. & Lu, K.-H. Receptor Guanylyl Cyclases in Inka Cells
355 Targeted by Eclosion Hormone. *Biol sc* **106**, 13371-76 (2009).
- 356 9. Chang, J. C., Yang, R. B., Chen, Y. H. & Lu, K. H. A novel guanylyl cyclase receptor, BdmGC-1, is
357 highly expressed during the development of the oriental fruit fly *Bactrocera dorsalis* (Hendel).
358 *Insect Mol Biol* **15**, 69–77 (2006).
- 359 10. Kingan, T. G., Gray, W., Žitňan, D. & Adams, M. E. Regulation of Ecdysis-Triggering Hormone
360 Release by Eclosion Hormone. *J Exp Biol* **200**, 3245-3256 (1997).
- 361 11. Žitňan, D., *et al.* Steroid induction of a peptide hormone gene leads to orchestration of a
362 defined behavioral sequence. *Neuron* **23**, 523-535 (1999).
- 363 12. Arakane, Y. *et al.* Functional analysis of four neuropeptides, EH, ETH, CCAP and bursicon, and
364 their receptors in adult ecdysis behavior of the red flour beetle, *Tribolium castaneum*. *Mech*
365 *Dev* **125**, 984–995 (2008).
- 366 13. Krüger, E., Mena, W., Lahr, E. C., Johnson, E. C. & Ewer, J. Genetic analysis of Eclosion
367 hormone action during *Drosophila* larval ecdysis. *Development* **142**, 4279–4287 (2015).
- 368 14. Mcnabb, S. L. *et al.* Disruption of a Behavioral Sequence by Targeted Death of Peptidergic
369 Neurons in *Drosophila*. *Neuron* **19**, 813-823 (1997).
- 370 15. Cullen, D. A. *et al.* From Molecules to Management: Mechanisms and Consequences of Locust
371 Phase Polyphenism. *Advances in Insect Physiol* **53**, 167–285 (2017).
- 372 16. Verbakel, L. *et al.* Prothoracostatic activity of the ecdysis-regulating neuropeptide
373 crustacean cardioactive peptide (CCAP) in the desert locust. *Int J Mol Sci* **22**, 13465 (2021).

- 374 17. Livak, K. J. & Schmittgen, T. D. Analysis of relative gene expression data using real-time
375 quantitative PCR and the $2^{-\Delta\Delta CT}$ method. *Methods* **25**, 402–408 (2001).
- 376 18. Verlinden, H. *et al.* First draft genome assembly of the desert locust, *Schistocerca gregaria*.
377 *F1000Res* **9**, 775 (2020).
- 378 19. Petersen, T. N., Brunak, S., von Heijne, G. & Nielsen, H. SignalP 4.0: discriminating signal
379 peptides from transmembrane regions. *Nat Methods* **8**, 785–6 (2011).
- 380 20. Cullen, D. A. *et al.* Sexual repurposing of juvenile aposematism in locusts. *PNAS* **119**,
381 e2200759119 (2022).
- 382 21. Fujita, N. & Yoshida, M. Efficient folding of the insect neuropeptide eclosion hormone by
383 protein disulfide isomerase. *J Biochem* **130**, 575–580 (2001).
- 384 22. Veenstra, J. A. The contribution of the genomes of a termite and a locust to our
385 understanding of insect neuropeptides and neurohormones. *Front Physiol* **5**, 1–22 (2014).
- 386 23. Žitňan, D. & Daubnerová, I. Eclosion Hormone. *Handbook of Hormones: Comparative*
387 *Endocrinology for Basic and Clinical Research* **459**, e76-2 (2015).
- 388 24. Lucas, K. A. *et al.* Guanylyl cyclases and signaling by cyclic GMP. *Pharmacol Rev* **52**, 375–413
389 (2000).
- 390 25. De Léan, A., McNicoll, N. & Labrecque, J. Natriuretic peptide receptor A activation stabilizes a
391 membrane-distal dimer interface. *Journal of Biological Chemistry* **278**, 11159–11166 (2003).
- 392 26. Bongrand, P. Ligand-receptor interactions. *Rep. Prog. Phys.* **62**, 921–968 (1999).
- 393 27. Hughes, M. E., Mesoy, S. M., Capes, E. & Lummis, S. C. R. Many Proline Residues in the
394 Extracellular Domain Contribute to Glycine Receptor Function. *ACS Chem Neurosci* **11**, 2658–
395 2665 (2020).
- 396 28. Truman, J. W. & Copenhaver, P. F. The larval eclosion hormone neurons in *Manduca sexta*:
397 Identification of the brain-proctodeal neurosecretory system. *J exp. Biol* **147**, 457-470 (1989).
- 398 29. Žitňan, D., *et al.* Molecular cloning and function of ecdysis-triggering hormones in the
399 silkworm *Bombyx mori*. *J Exp Biol* (2002) **205**, 3459–3473.
- 400 30. Li, Z., Ye, Q., Lyu, Z. & Lin, T. RNA interference of eclosion hormone gene reveals its roles in
401 the control of ecdysis behavior in *Heortia vitessoides*. *Arch Insect Biochem Physiol* **105**,
402 e21726 (2020).
- 403 31. Hewes, R. S. & Truman, J. W. The Roles of Central and Peripheral Eclosion Hormone Release in
404 the Control of Ecdysis Behavior in *Manduca sexta*. *J Comp Physiol A* **168**, 697-707 (1991).
- 405 32. Feng Q, Liu M, Cheng Y & Wu X. Comparative Transcriptome Analysis Reveals the Process of
406 Ovarian Development and Nutrition Metabolism in Chinese Mitten Crab, *Eriocheir Sinensis*.
407 *Front Genet.* **24**, 13:910682 (2022).
- 408 33. Wang, Z. *et al.* Comparative transcriptomic characterization of the eyestalk in Pacific white
409 shrimp (*Litopenaeus vannamei*) during ovarian maturation. *Gen Comp Endocrinol* **274**, 60–72
410 (2019).

- 411 34. Gijbels, M., Lenaerts, C., Vanden Broeck, J. & Marchal, E. Juvenile Hormone receptor Met is
412 essential for ovarian maturation in the desert locust, *Schistocerca gregaria*. *Sci Rep* **9**, 10797
413 (2019).
- 414 35. Holtof, M. *et al.* Crucial role of juvenile hormone receptor components methoprene-tolerant
415 and taiman in sexual maturation of adult male desert locusts. *Biomolecules* **11**, 1–21 (2021).
- 416 36. Gijbels, M. *et al.* Precocious downregulation of krüppel-homolog 1 in the migratory locust,
417 *Locusta migratoria*, gives rise to an adultoid phenotype with accelerated ovarian development
418 but disturbed mating and oviposition. *Int J Mol Sci* **21**, 1–24 (2020).
- 419 37. Sugahara, R. & Tanaka, S. Yellowing and YPT gene expression in the desert locust, *Schistocerca*
420 *gregaria*: Effects of developmental stages and fasting. *Arch Insect Biochem Physiol* **101**,
421 e21551 (2019).
- 422
- 423


```

Schgr-EHR 1223 TSGNKFLEDNSRSTFPQTLREARSLDPLPDYDSTNVGHLQLNLQVPKRSSRSLENCVGGSGKLVPAHQFS
BdmGC-1 1195 DSYTGVRSSGAST.....HSRYEESTLSGSENE...ELT
BdmGC-1B 1214 .....
consensus * *** ** * *

```

```

Schgr-EHR 1293 SERCHAVNNNFPNGDAILLSPQSNVCGGSSSTDDIQTPLLQNFSDIDETITVKRQLRRGKSGTEPLPDFH
BdmGC-1 1227 SWQRQRRP.....SSVPTANTPLLNH.....
BdmGC-1B 1214 .....
consensus * * *** **** *

```

```

Schgr-EHR 1363 PDKRWSLEEMPGNDANVNGHSHKTLARNSIRSWLAGLFNGNGLRTSDASLRKGIHSGYSDLQSEKESIV
BdmGC-1 1249 .....VEIT
BdmGC-1B 1214 .....IT
consensus .....

```

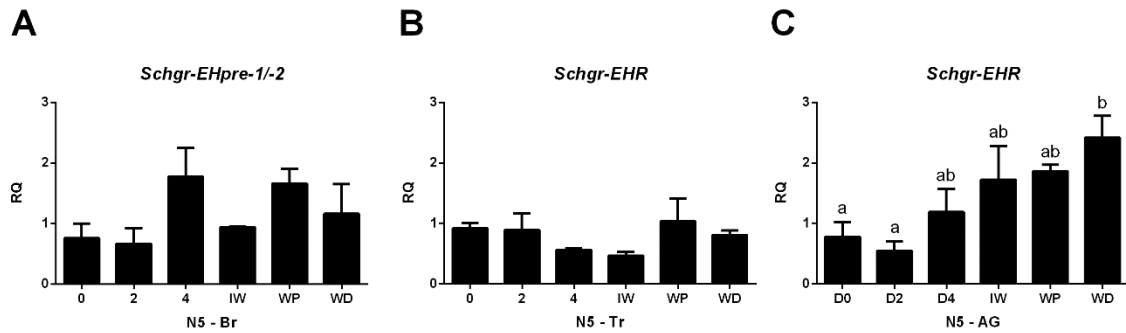
441

442 **Sequence alignment of the putative *Schgr*-EHR** with the functionally characterized *Bacdo*-EHR. The
443 amino acid position is indicated at the left. Identical residues between the aligned sequences are
444 highlighted in black and an exclamation mark (!), and conservatively substituted residues in grey and
445 an asterisk (*). Dots indicate gaps that are introduced to maximize similarities in the alignment.
446 Abbreviations: *Schgr* = *Schistocerca gregaria*, *BdmGC*-1(B) = *Bactrocera dorsalis* membrane guanylyl
447 cyclase 1(β) (AY125819.1 and ACQ90240.1), ECD = extracellular ligand-binding domain, TM =
448 transmembrane segment, PKHD = Pseudokinase homology domain, CYCc = Adenylyl-/ guanylyl
449 cyclase, catalytic domain type c.

450

451

452 **Figure 3:**
453

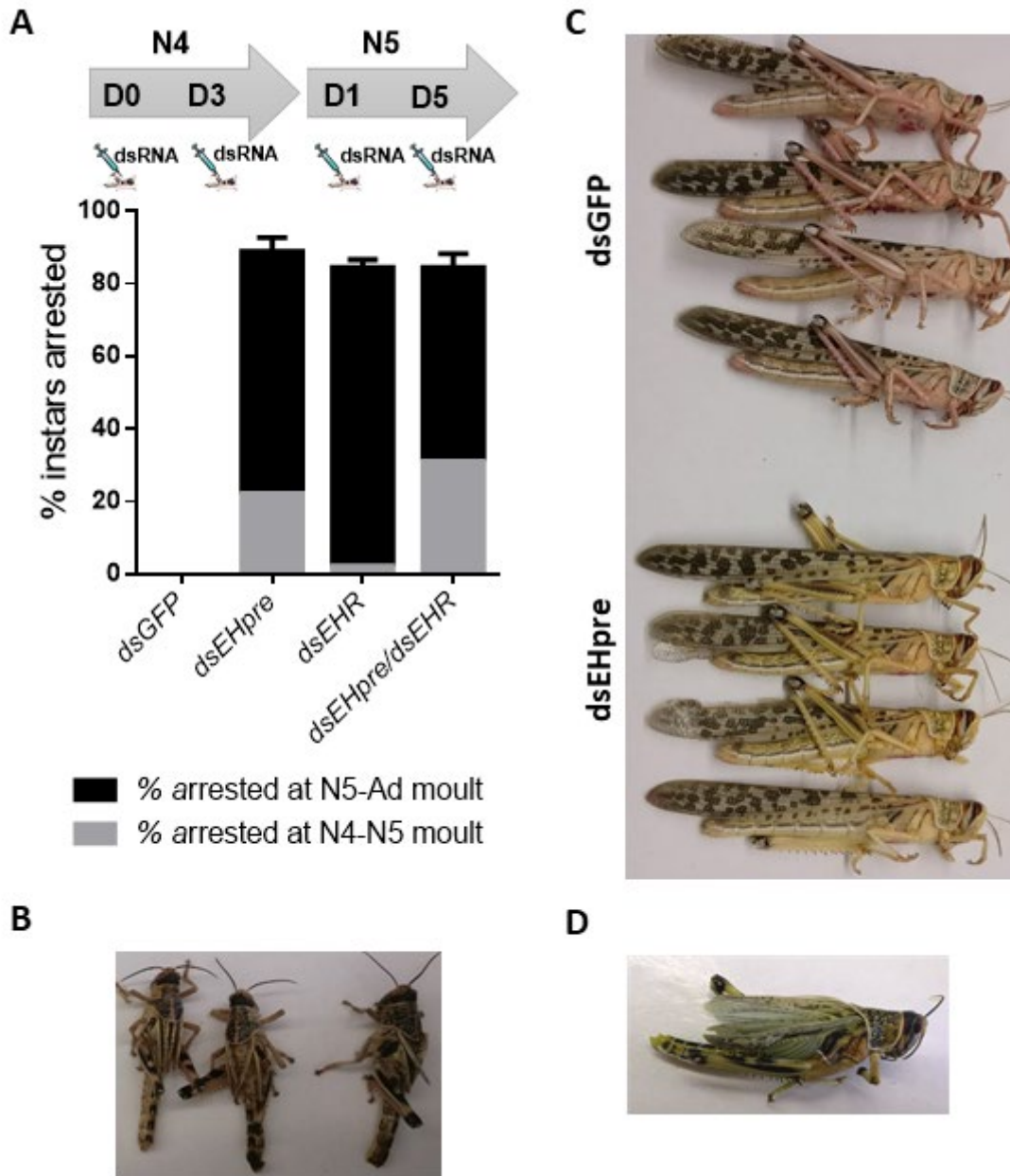


454

455 **Temporal expression profile of *Schgr-EHpre-1/-2* and *Schgr-EHR* in the fifth nymphal instar (N5) of**
456 ***S. gregaria* nymphs.** Using qRT-PCR, (A) the relative transcript levels of *Schgr-EHpre-1/-2* were
457 measured in the brain and the relative *Schgr-EHR* transcript levels were measured, respectively, in (B)
458 trachea and (C) abdominal ganglia, at different time points during N5. The data represent means \pm
459 S.E.M. of five independent pools of three nymphs, run in duplicate and normalized to the expression
460 of reference genes: *Schgr-EHpre* transcript levels were normalized to *RP-49* and *GAPDH* transcript
461 levels, while *Schgr-EHR* transcript levels were normalized to *β -Actin*, *CG13220* and *GAPDH* transcript
462 levels. Significant differences were calculated by One-way ANOVA, followed by a Dunnett's Test.
463 Abbreviations: *Schgr* = *Schistocerca gregaria*, *EHpre* = *Ecdysis hormone precursor*, *EHR* = *Ecdysis*
464 *hormone receptor*, IW = inter-wing distance of at least 1.8 mm, WP = weight peak, WD = weight
465 decrease, RQ = relative quantity.

466

467 **Figure 4:**
468



469

470

471 **Phenotypic effects of *dsEHpre* and/or *dsEHR* injections in *Schistocerca gregaria*.** A) Percentage of
472 nymphs arrested at the last nymphal-nymphal (N4-N5) and at the nymphal-adult (N5-Ad) molt.

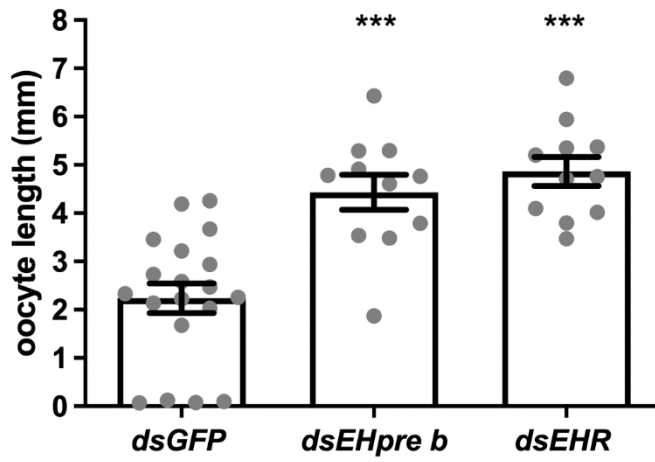
473 Phenotypes: B) Nymphs arrested at ecdysis, C) Yellowed coloration in *dsEHpre*-injected adults at

474 Add1, D) Supernumerary sixth instar nymph.

475

476 **Figure 5:**

477

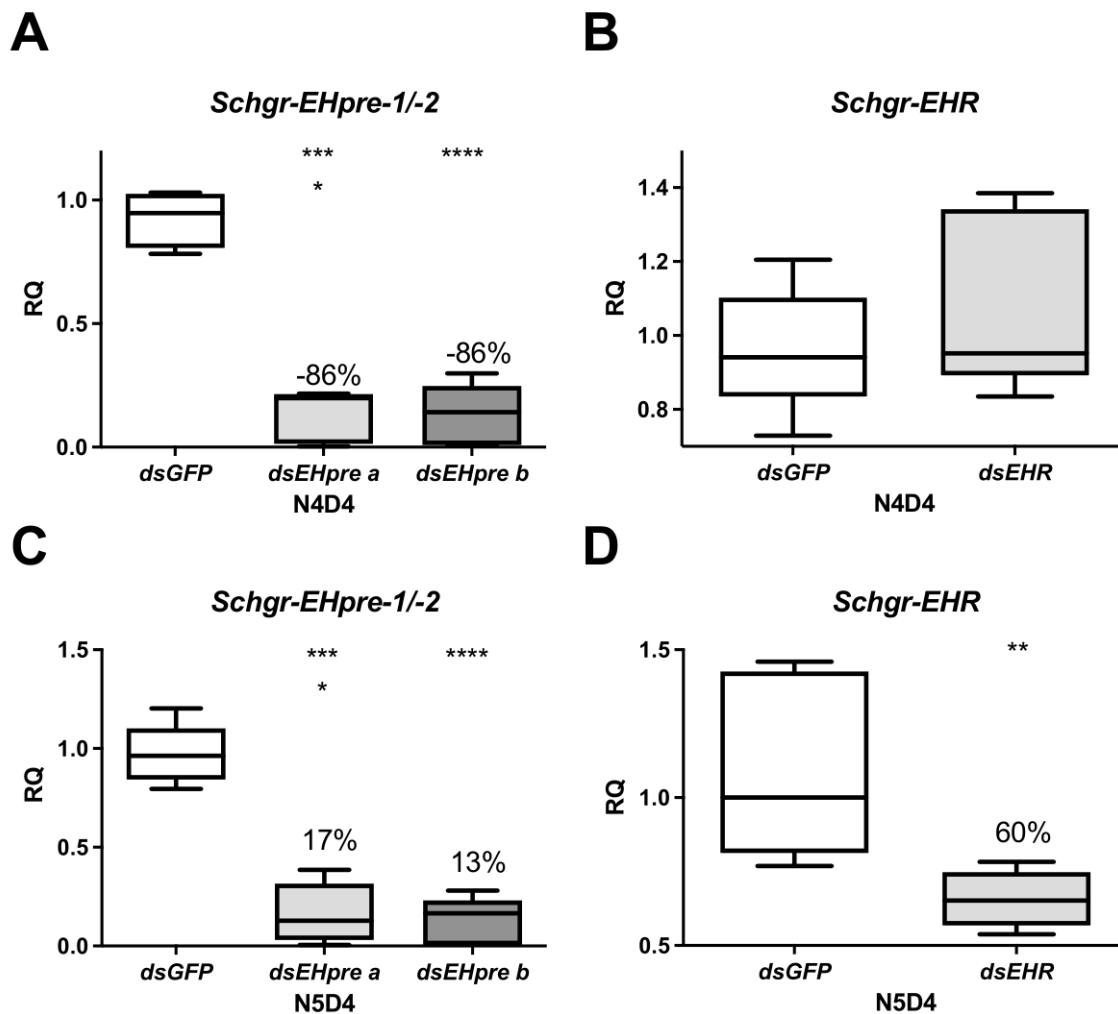


478

479

480 **Effect of *Schgr-EHpre* or *Schgr-EHR* depletion on oocyte size at 10-day-after eclosion.** Significant
481 differences ($p < 0.05$, $p < 0.1$ and $p < 0.001$) are indicated by asterisks (*, ** and ***, respectively) and
482 were calculated by One-way ANOVA, followed by a Dunnett's Test.}

483



486

487

488 **Figure S1:**

489 **Relative quantities of *Schgr-EHpre-1/-2* and *Schgr-EHR* transcripts** in brain and trachea, respectively,
 490 as measured in *S. gregaria* nymphs at N4D4 and N5D4. *dsGFP* and *dsEHpre* or *dsEHR* were injected at
 491 N4D0. Boost injections were administered at N4D4, N5D1 and N5D5. A) RNAi-mediated knockdown
 492 caused by administering *dsEHpre-a* or *-b* constructs on *Schgr-EHpre-1/-2* transcript levels at N4D4. B)
 493 RNAi-mediated knockdown caused by administering *dsEHR* on *Schgr-EHR* transcript levels at N4D4. C)
 494 RNAi-mediated knockdown caused by administering *dsEHpre-a* or *-b* constructs on *Schgr-EHpre-1/-2*
 495 transcript levels at N5D4. D) RNAi-mediated knockdown efficiency caused by administering *dsEHR* on
 496 *Schgr-EHR* transcript levels at N5D4. Significant differences ($p < 0.01$ and $p < 0.0001$) are indicated by
 497 asterisks (** and ****, respectively) and were calculated by One-way ANOVA, followed by a
 498 Dunnett's Test.

499

500 **Supplementary Table**

501 **Table S1:** Oligonucleotide sequences for primers used in cloning and sequence analysis of *Schgr-*
 502 *EHpre-1*, *Schgr-EHpre-2* and *Schgr-EHR*, for primers used for dsRNA construct creation and for
 503 primers used in qRT-PCR

cloning	Forward primer	Reverse primer
<i>Schgr-EHpre-1</i>	CGGCGATCCTCTCCTGTAGT	GCAGACGGACTTTATTGAGCC
<i>Schgr-EHpre-1_nested</i>	GTAGTAGACATGGCCCTCTGC	CGGCTACTCGAGTTTGCTGA
<i>Schgr-EHpre-2</i>	CCACCAGCACCACTTCACTA	CACGAGGGAGAGCAGGTAAC
<i>Schgr-EHpre-2_nested</i>	CTCTCTTACACAGAGATGGCCG	CTACTCGAGCTTGTTGAGGAGGG
<i>Schgr-EHR</i>	GTTCCAGACTGTAGCGCT	CATTCACCTGCAGATGGTGT
<i>Schgr-EHR_nested</i>	TCCACCATCCAGACAGTAGAC	GTTAAGATACTACACTACCTATTGGT
dsRNA	Forward primer	Reverse primer
<i>dsEHR</i>	TAATACGACTCACTATAGGGAGAAGTTGTGCTAA CCCCACCTG	TAATACGACTCACTATAGGGAGATTGCTCCTGT GATGCTCGT
<i>dsEHpre-a</i>	TAATACGACTCACTATAGGGAGAATGGCCCTCTG CCGTCC	TAATACGACTCACTATAGGGAGAACGGCCCCGAC ATCTTCTTA
<i>dsEHpre-b</i>	TAATACGACTCACTATAGGGAGAATGGCCGCCCG CCGCTG	TAATACGACTCACTATAGGGAGAGCGTTGGCGT CCGCTGGCG
<i>dsGFP</i>	TAATACGACTCACTATAGGGAGAAAGGTGATGCT ACATACGGAA	TAATACGACTCACTATAGGGAGAATCCCAGCAG CAGTTACAAAC
qRT-PCR	Forward primer	Reverse primer
<i>Schgr-EHpre-1</i>	TGGTGGCAGCAGTCTACCT	ACAGCTGGCCCTCGAAATAC
<i>Schgr-EHpre-2</i>	AGCGTCTGCATTCACAACTG	CTCGAGCTTGTTGAGGAAGG
<i>Schgr-EHR-1</i>	TTGCATGAGCTTAGGCAGTG	TGGAGGATGCCCTTATGAAC
<i>Schgr-EHR-2</i>	ACAACCTATTCCGCGAACCT	GTGCCTGAAGACAACCTTTGA

<i>Schgr</i> - <i>RP49</i>	CGCTACAAGAAGCTTATGAGGTCAT	CCTACGGCGCACTTCTGTTG
<i>Schgr</i> - β - <i>Actin</i>	AATTACCATTGGTAACGAGCGATT	TGCTCCATACCCAGGAATGA
<i>Schgr</i> - <i>GAPDH</i>	GTCTGATGACAACAGTGCAT	GTCCATCACGCCACAACCTTC
<i>Schgr</i> - <i>CG13220</i>	TGTTCAGTTTTGGCTGTTCTGA	ACTGTTCTCCGGCAGAATGC

504 Abbreviations : *Schgr* = *Schistocerca gregaria*, *EHpre* = Eclosion hormone precursor, *EHR* = Eclosion
505 hormone receptor, *RP49* = ribosomal protein 49, *GAPDH* = Glyceraldehyde-3-phosphate
506 dehydrogenase.

507